Cell surface expression of the stress response chaperone GRP78 enables tumor targeting by circulating ligands

Marco A. Arap,[1,3] Johanna Lahdenranta,[1,3] Paul J. Mintz,[1] Amin Hajitou,[1] Álvaro S. Sarkis,[2] Wadih Arap,[1,*] and Renata Pasqualini[1,*]

[1]The University of Texas M.D. Anderson Cancer Center, Houston, Texas 77030
[2]University of São Paulo Medical School, São Paulo, SP 05403, Brazil
[3]These authors contributed equally to this work.
*Correspondence: warap@mdanderson.org (W.A.); rpasqual@mdanderson.org (R.P.)

Summary

We have recently identified glucose-regulated protein-78 (GRP78) as a relevant molecular target expressed in metastatic tumors by fingerprinting the circulating repertoire of antibodies from cancer patients. Here we design and evaluate a ligand-receptor system based on the tumor cell membrane expression of GRP78. We show that GRP78 binding peptide motifs target tumor cells specifically in vivo and in human cancer specimens ex vivo. Moreover, synthetic chimeric peptides composed of GRP78 binding motifs fused to a programmed cell death-inducing sequence can suppress tumor growth in xenograft and isogenic mouse models of prostate and breast cancer. Together, these preclinical data validate GRP78 on the tumor cell surface as a functional molecular target that may prove useful for translation into clinical applications.

Introduction

The membrane compartment of cells in tumors contains many receptors that are required for their survival. In particular, members of the unfolded protein response (Kaufman, 1999; Lee, 2001; Reddy et al., 2003), such as the glucose-regulated protein and the heat shock protein families, are candidate targets on the tumors; the presence and functionality of this subset of chaperone proteins in signal transduction, drug resistance, apoptosis, and immunomodulation has recently begun to be recognized (Beere et al., 2000; Lee, 2001; Kamal et al., 2003; Mintz et al., 2003; Neckers and Lee, 2003; Nicchitta, 2003; Ravagnan et al., 2001; Reddy et al., 2003; Shin et al., 2003).

By screening combinatorial peptide libraries, we identified one such glucose-regulated protein family member, glucose-regulated protein-78 kDa (GRP78), as a tumor antigen through epitope mapping of the humoral immune response from cancer patients (Mintz et al., 2003). Because GRP78 confers a protective cellular response against stress conditions present in solid tumors (Jamora et al., 1996; Koong et al., 1994; Li et al., 1992; Miyake et al., 2000; Reddy et al., 2003; Sugawara et al., 1993), we hypothesized that GRP78 expressed on the cell surface of cancer cells (Mintz et al., 2003; Shin et al., 2003) could serve as a functional receptor in vivo. In order to evaluate whether GRP78 ligands would allow targeting of solid tumors, we devised experiments to assess GRP78-based protein-protein interactions in solid phase, cell lines, xenograft and isogenic tumor models in mice, and human cancer specimens.

Here we introduce two ligand peptides that can specifically (1) bind to GRP78 in a cell-free system, (2) target cell surfaces in vitro, (3) home in vivo to tumors in mouse models of breast and prostate cancer, (4) suppress tumor growth when synthesized as a fusion chimeric peptide with a proapoptotic sequence, and finally (5) bind to patient-derived cancer samples. Together, these data indicate that GRP78 is a functional molecular target on tumor cell surfaces in vivo. This ligand-receptor system may yield targeted therapy applications and should be considered for validation against primary and metastatic tumors.

Results

Choice of GRP78 binding peptides and initial evaluation of targeting vectors

To design the targeting vectors that were used here, we evaluated a panel of four predicted GRP78 binding motifs (Blond-Elguindi et al., 1993) in phage binding assays. Among the consensus peptide motifs tested in our phage-targeting system, the ligand peptides WIFPWIQL and WDLAWMFRLPVG showed the best targeting activity and specificity to GRP78, relative to control proteins (Supplemental Figure S1 at http://www.cancercell.org/cgi/content/full/6/3/275/DC1). Given the binding

---

S I G N I F I C A N C E

Several lines of evidence indicate that glucose-regulated stress response proteins can (1) serve as functional chaperones on the tumor cell surface, (2) confer tumor selectivity on specific inhibitors, and (3) regulate multiple signaling pathways related to apoptosis, immune function, and drug resistance. Thus, we sought to evaluate whether glucose-regulated proteins would be suitable receptors for systemic targeting of tumors. Our results illustrate the ability of one such glucose-regulated protein, GRP78, to function as a membrane-associated molecular chaperone that enables tumor targeting. Given the promising therapeutic data in experimental models and the presence of the receptor in patient-derived samples, this system should be considered for targeted drug development.
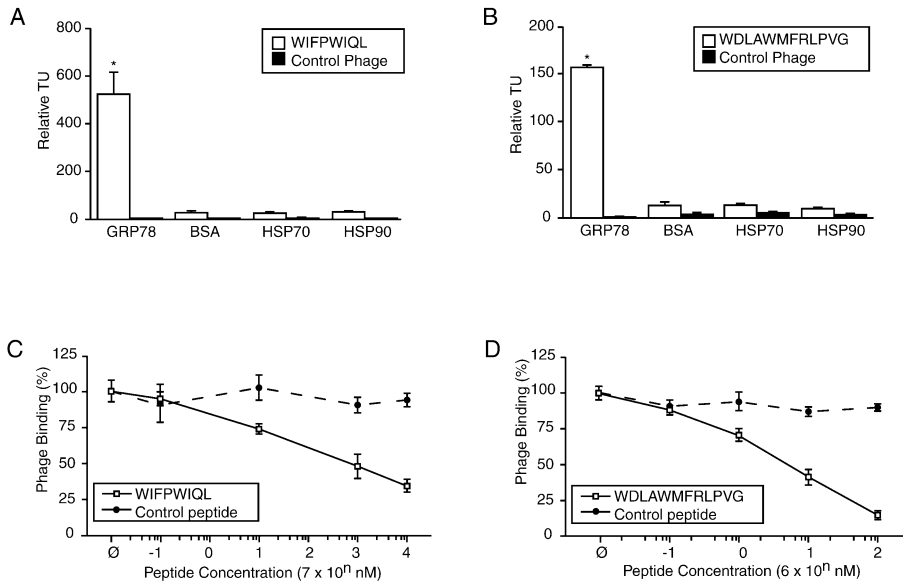
Figure 1. Filamentous phage clones displaying WIFPWIQL and WDLAWMFRLPVG peptides bind specifically to GRP78

GRP78, HSP70, HSP90, or BSA was coated on microtiter wells at 10 μg/ml and incubated with either WIFPWIQL-phage (**A**) or WDLAWMFRLPVG-phage (**B**). An insertless phage (fd-tet) served as the negative control. Phage input was 10^9 TU per well. Results are expressed as mean ± standard error of the mean (SEM) of triplicate wells. Binding inhibition of WIFPWIQL-phage (**C**) and WDLAWMFRLPVG-phage (**D**) to immobilized GRP78 was obtained by the addition of the corresponding synthetic peptides. Microtiter wells were coated with GRP78 at 10 μg/ml, and phage clones were incubated with increasing concentrations of synthetic cognate or control peptides. Experiments were performed three times with similar results. *Student's t test, $p < 0.01$.

properties of these peptides, we decided to use fUSE5-derived phage vector constructs displaying the GRP78 binding motifs WIFPWIQL and WDLAWMFRLPVG as fusion peptides to the minor coat protein pIII (Smith and Scott, 1993) for further experiments.

Cell-free binding of ligand peptides to immobilized GRP78 is specific

We evaluated binding of WIFPWIQL-phage (Figure 1A) and of WDLAWMFRLPVG-phage (Figure 1B) to recombinant GRP78 in microtiter wells. Both WIFPWIQL-phage and WDLAWMFRLPVG-phage bound significantly more to GRP78 in vitro than to control proteins, including heat shock protein 70 (HSP70), heat shock protein 90 (HSP90), and bovine serum albumin (BSA). Moreover, WIFPWIQL-phage (870-fold; Student's t test, $p < 0.001$) and WDLAWMFRLPVG-phage (260-fold; Student's t test, $p < 0.001$) bound significantly more to immobilized GRP78 in vitro than did a negative control phage displaying no insert (fd-tet). We observed a dose-dependent inhibition of WIFPWIQL-phage (Figure 1C) and WDLAWMFRLPVG-phage (Figure 1D) binding to GRP78 by the corresponding synthetic peptides; control peptides with unrelated sequences had no detectable effect. Together, these data show that ligand peptides displayed in a filamentous phage specifically bind to immobilized GRP78.

GRP78 binding peptides target cell surfaces in vitro

Having determined the specificity of GRP78 binding peptides to the immobilized protein in a cell-free system, we next evaluated binding to human DU145 prostate cancer cells (Figure 2). Binding of filamentous phage clones displaying WIFPWIQL (Figure 2A) and WDLAWMFRLPVG (Figure 2B) to intact tumor cells was performed by using an aqueous-organic phase separation assay (Giordano et al., 2001). Each of the GRP78 binding phage clones or insertless negative control phage was incubated with DU145 cells. Binding to DU145 cells was at least 30-fold higher (Student's t test, $p < 0.001$) with WIFPWIQL-phage or WDLAWMFRLPVG-phage compared to fd-tet phage. The GRP78-mediated interaction of either WIFPWIQL-phage (Figure 2A) or WDLAWMFRLPVG-phage (Figure 2B) to DU145 cell surfaces was specific given that an anti-GRP78 polyclonal antibody (Fig-

ure 2, left panels), recombinant GRP78 in solution (Figure 2, middle panels), or the corresponding synthetic peptides (Figure 2, right panels) inhibited binding. Control isotypic antibodies, unrelated control proteins, and peptides did not affect binding of the GRP78 binding phage. These results indicate that GRP78 binding peptides can specifically target cell surfaces.

GRP78 binding peptides undergo cell internalization

Next, we evaluated whether GRP78 would mediate internalization of a ligand into cells. We used the DU145 line as representa-
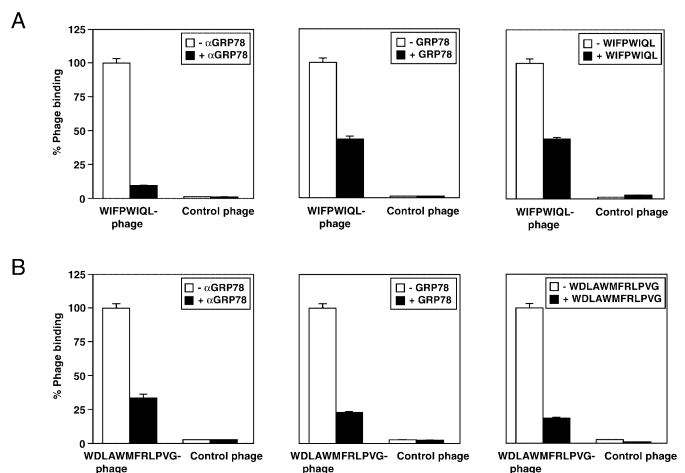

Figure 2. GRP78-targeted phage binding to tumor cells is specific

The BRASIL method (Giordano et al., 2001) was applied to test the binding of WIFPWIQL-phage, WDLAWMFRLPVG-phage, or control insertless phage to the human prostate cancer-derived DU145 cells. Transducing unit counts of the GRP78 binding clones without inhibition was set to 100% in each case. Results are expressed as mean ± SEM of triplicates. Binding inhibition of both WIFPWIQL-phage (**A**) and WDLAWMFRLPVG-phage (**B**) was evaluated by the addition of a polyclonal anti-GRP78 or an unrelated control antibody (left panels), recombinant GRP78 (middle panels), and soluble synthetic peptides (right panels).

tive human prostate cancer-derived cells expressing GRP78 on the cell surface (Mintz et al., 2003) and GRP78 binding phage as targeted ligands. Each phage clone or control phage was incubated with cells for 4 hr at 37°C. Cells were washed to remove noninternalized phage, permeabilized, and stained with an anti-bacteriophage antibody. A Cy^3-conjugated secondary antibody was used to detect the presence and localization of phage particles. GRP78-targeted phage internalization was temperature dependent and time dependent, being detectable at 8 hr and peaking at 24 hr (data not shown). Both WIFPWIQL-phage and WDLAWMFRLPVG-phage were internalized into DU145 cells; only background fluorescence was observed when nonpermeabilized cells or nontargeted control phage (Figure 3A) were used as negative controls. These results indicate that the binding peptides WIFPWIQL and WDLAWMFRLPVG can mediate the internalization of GRP78-targeted phage into cells. Moreover, in order to show that the internalization of GRP78 binding ligands can also occur outside of the context of targeted phage constructs, we have also evaluated cell killing in vitro by the synthetic GRP78 binding peptide WDLAWMFRLPVG fused to the programmed cell death-inducing domain $_D(KLAKLAK)_2$, an amphipatic α helix-forming antimicrobial peptide (Javadpour et al., 1996) that preferentially disrupts eukaryotic mitochondrial membranes upon receptor-mediated internalization (Arap et al., 2002b; Ellerby et al., 1999; Kolonin et al., 2004; Zurita et al., 2004). Increasing concentrations of either WDLAWMFRLPVG-GG-$_D(KLAKLAK)_2$ or negative control peptides [an equimolar admixture of WDLAWMFRLPVG plus $_D(KLAKLAK)_2$] were incubated with DU145 cells at 37°C, and viability was assessed over time. To gain insight into the mechanism of peptide internalization, we also determined whether endocytosis and GRP78 recycling could be affected by ATPase inhibitors (Schmid and Carter, 1990). Treatment of cells resulted in a dose-dependent decrease of cell viability with WDLAWMFRLPVG-GG-$_D(KLAKLAK)_2$ relative to controls, and the apoptosis is inhibited by sodium azide (Figure 3B). Taken together, these data suggest that cell internalization of GRP78 binding ligands is likely mediated by an active GRP78-dependent mechanism.

GRP78 binding phage home to tumors upon systemic administration

To determine the ability of GRP78 binding phage clones to home to tumors in vivo, we administered WIFPWIQL-phage, WDLAWMFRLPVG-phage, or control insertless phage intravenously to nude mice bearing DU145-derived human prostate cancer xenografts (Figure 4). After 24 hr, the mice were sacrificed, and the tumors and several control organs were collected and analyzed for phage staining. We observed strong tumor staining for each GRP78 binding phage clone, while only background staining was detected in control organs; moreover, negative control phage was not detected in tumors or several control organs (Figure 4). It is of note that, as part of the reticuloendothelial system, hepatic and splenic tissues clear circulating particles (such as phage) nonspecifically and independently of the peptides displayed. These data show that human prostate cancer-derived tumor xenografts growing in nude mice can be targeted by GRP78 binding phage in vivo.

GRP78-targeted proapoptotic synthetic peptides suppress tumor growth

We next sought to establish whether synthetic chimeras composed of the GRP78 binding peptides fused to the programmed
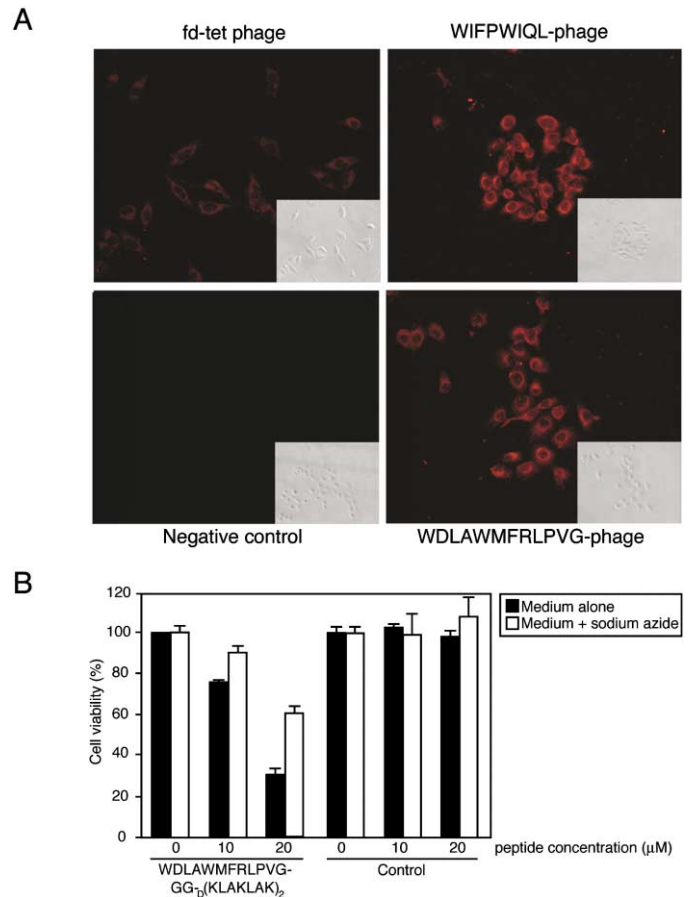

Figure 3. GRP78-targeted peptides can mediate ligand-receptor cell internalization

WIFPWIQL-phage, WDLAWMFRLPVG-phage, or control insertless phage were incubated with human prostate cancer-derived DU145 cells for 4 hr at 37°C to allow phage internalization. Internalized phage clones were detected with an anti-phage antibody after cell permeabilization (see the Experimental Procedures).
A: WIFPWIQL-phage and WDLAWMFRLPVG-phage were internalized into DU145 cells relative to cells incubated with an insertless control phage; cells incubated with no phage are also shown to assess staining background.
B: DU145 cells were incubated with increasing concentrations (up to 20 μM) of the GRP78-targeted proapoptotic peptide WDLAWMFRLPVG-GG-$_D(KLAKLAK)_2$ or negative control peptides [an equimolar mixture of WDLAWMFRLPVG plus $_D(KLAKLAK)_2$] in the presence or absence of 20 mM sodium azide. As described in the Experimental Procedures, viability determined by optical absorbance using a cell proliferation detection reagent without any peptide treatment was set to 100%.

cell death-inducing domain (Arap et al., 2002b; Ellerby et al., 1999; Kolonin et al., 2004; Zurita et al., 2004) would have antitumor effects in vivo. We used nude mice bearing DU145-derived human prostate cancer xenografts (Figures 5A and 5B) or immunocompetent Balb/c mice bearing EF43-*fgf4*-derived isogenic tumors (Figures 5C and 5D). Mice received weekly doses of targeted peptides or controls. Posttreatment mean tumor volumes in the groups treated with the targeted GRP78 binding chimeric peptides WIFPWIQL-GG-$_D(KLAKLAK)_2$ (Figures 5A and 5C) or WDLAWMFRLPVG-GG-$_D(KLAKLAK)_2$ (Figures 5B and 5D) were significantly lower (Student's t test, p < 0.002 in each case) relative to controls treated with vehicle alone. The sup-
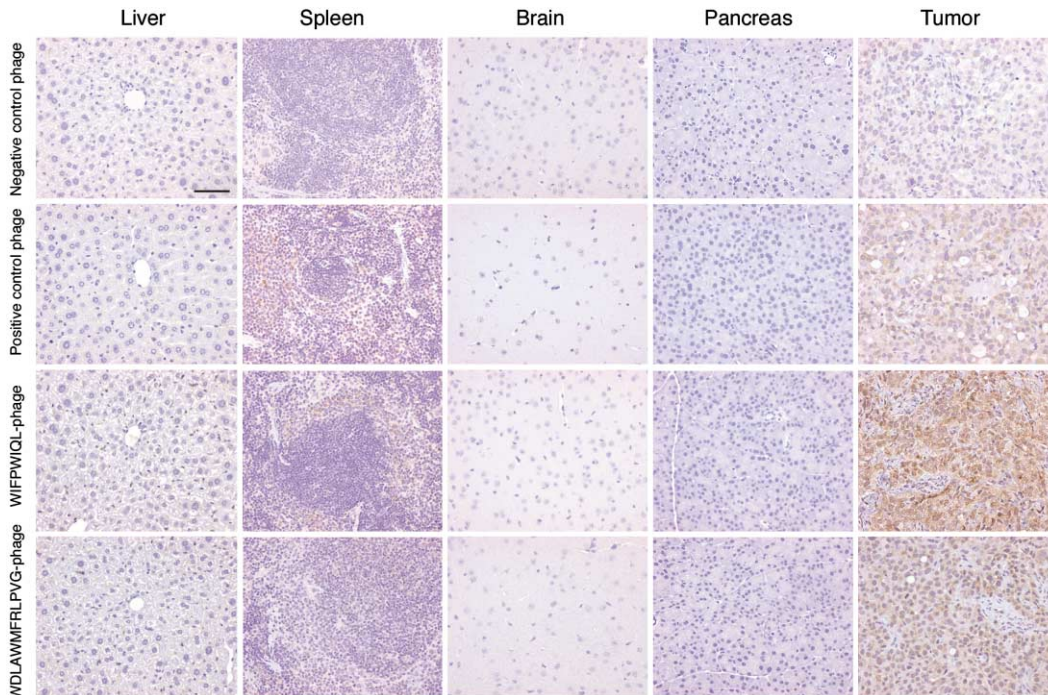
Figure 4. Immunohistochemical staining of GRP78-targeted phage after systemic administration into human prostate cancer xenograft-bearing mice

Insertless phage fd-tet (negative control), RGD-4C phage (positive control), or phage displaying the GRP78 binding peptides WIFPWIQL and WDLAWMFRLPVG were intravenously administered into mice bearing DU145-derived prostate carcinoma xenografts. Phage clones were allowed to circulate for 24 hr, and tissues were recovered and stained as described in the Experimental Procedures. A strong phage staining was observed with WIFPWIQL-phage or WDLAWMFRLPVG-phage in tumor xenografts. Little or no staining was observed either with fd-tet phage or with GRP78 binding phage clones in control organs. Scale bar, 100 μm.

pression of tumor growth was slightly less efficient in mice bearing EF43-*fgf4* tumors, likely reflecting the aggressiveness of the model. Tumors in mice treated by equimolar mixtures of either WIFPWIQL plus $_D$(KLAKLAK)$_2$ or WDLAWMFRLPVG plus $_D$(KLAKLAK)$_2$ behaved similarly to those tumors in mice that received vehicle only, indicating that untargeted $_D$(KLAKLAK)$_2$ with GRP78 binding peptides had no detectable effect on tumor growth.

GRP78-mediated cell apoptosis in vitro does not model therapeutic in vivo targeting
To address whether the presence of GRP78 as a target on the cell surface is related to the unfolded protein response (Kaufman, 1999; Lee, 2001; Reddy et al., 2003) rather than an inherent feature of tumors per se, we examined both malignant and nonmalignant cells in vitro. First, we performed fluorescence-activated cell surface (FACS) analysis of a representative panel of human and mouse cell lines, including tumor cells of epithelial and nonepithelial origin, as well as nonmalignant cells. We detected positive surface staining, indicating broad membrane expression of GRP78 in all the lines cultured in vitro (data not shown). Next, to confirm the functional relevance of the surface expression of GRP78, we have evaluated targeted cell killing in vitro by GRP78 binding peptides chimerized with the $_D$(KLAKLAK)$_2$ proapoptotic motif (Arap et al., 2002b; Ellerby et al., 1999; Kolonin et al., 2004; Zurita et al., 2004). Consistently, as cultured cells grown in vitro appear to express GRP78 at the membrane level, we have observed programmed cell death in all cell lines

studied regardless of whether or not they were tumor cells (Supplemental Figure S2 at http://www.cancercell.org/cgi/content/full/6/3/275/DC1). These contrasting results indicate that GRP78-mediated cell death in vitro (Supplemental Figure S2) does not recapitulate the selective induction of tumor cell apoptosis in vivo (Figure 5); such paradox might be due to the upregulation of stress response proteins (such as GRP78, one of the hallmarks of the unfolded protein response), which is likely to occur in cells grown in vitro, outside of their optimal in vivo physiological conditions. In fact, very recently it became clear that *GRP78* promoter-driven expression of a reporter transgene is undetectable in all the major organs evaluated in adult mice (such as liver, spleen, kidney, brain, lung, heart, and pancreas); in contrast, the *GRP78* promoter is highly active in tumors (Dong et al., 2004). Consistently, we have detected programmed cell death induction by TUNEL staining in DU145-derived tumor xenografts but not in control organs, in agreement with *GRP78* promoter studies in tumor-bearing mice (Supplemental Figure S3; Dong et al., 2004).

GRP78 binding phage clones recognize human prostate cancer samples
Because we found GRP78 expression to be high in human prostate cancer (Mintz et al., 2003), we used phage overlay assays (Arap et al., 2002a; Zurita et al., 2004) to determine whether the GRP78-targeting phage would bind to bone marrow metastases from patient-derived prostate cancer. To evaluate whether the GRP78 binding phage could inhibit the anti-GRP78
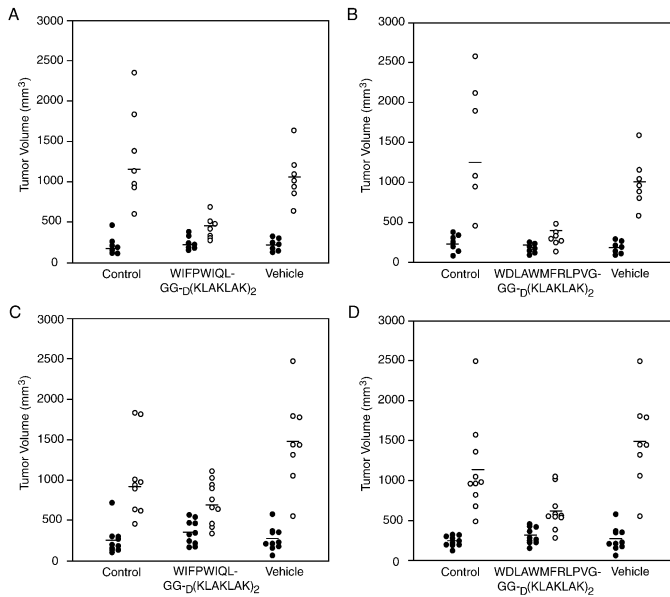
Figure 5. Treatment of tumor-bearing mice with GRP78-targeted proapoptotic peptides

We used nude mice bearing DU145-derived human prostate cancer xenografts (**A** and **B**) or Balb/c mice bearing EF43-*fgf4* murine breast carcinoma tumors (**C** and **D**). The synthetic GRP78-targeted proapoptotic peptides WIFPWIQL-GG-$_D$(KLAKLAK)$_2$ and WDLAWMFRLPVG-GG-$_D$(KLAKLAK)$_2$ were used in each tumor model. Individual tumor volumes are represented before (filled circles) and after (open circles) treatment for the synthetic GRP78-targeted proapoptotic peptides WIFPWIQL-GG-$_D$(KLAKLAK)$_2$ (**A** and **C**) and WDLAWMFRLPVG-GG-$_D$(KLAKLAK)$_2$ (**B** and **D**). Controls used were vehicle alone and equimolar mixtures of unconjugated WIFPWIQL plus $_D$(KLAKLAK)$_2$ for **A** and **C** or WDLAWMFRLPVG plus $_D$(KLAKLAK)$_2$ for **B** and **D**. In each case, mean tumor volumes were significantly smaller (Student's t test, p < 0.001) in mice treated with the GRP78-targeted proapoptotic peptides relative to vehicle or to the corresponding control peptides.

Figure 6. Inhibition of anti-GRP78 antibody staining by GRP78 binding phage

Serial tissue sections of bone marrow metastases from human prostate cancer were incubated with the WIFPWIQL-phage, WDLAWMFRLPVG-phage, or negative control phage prior to adding an anti-GRP78 antibody to the sections. Strong staining was observed when the anti-GRP78 antibody was used with no phage (**A**), compared to a negative control antibody with the same isotype and concentration (**B**). Preincubation with WIFPWIQL-phage (**C**) or WDLAWMFRLPVG-phage (**D**) inhibited the staining by the anti-GRP78 antibody, whereas a negative control phage with no peptide did not affect the staining of the anti-GRP78 antibody (**E**). An eosin staining of the tumor is shown in **F**. Scale bar, 100 μm.

antibody staining, WIFPWIQL-phage, WDLAWMFRLPVG-phage, and negative control phage were overlaid on serial human tissue sections prior to adding the anti-GRP78 antibody or negative control antibody. Consistently, markedly reduced antibody staining was observed with each GRP78 binding phage clone but not with the negative control phage (Figure 6). Moreover, in a reverse experiment, each GRP78 binding phage or negative control phage was overlaid on serial human tissue sections. After extensive washing to remove nonspecific binding, samples were incubated with an anti-bacteriophage antibody. We observed a strong staining with the GRP78 binding phage clones and marked inhibition when an anti-GRP78 antibody was added to the slide; in contrast, no inhibition was observed with a control antibody (Figure 7).

Finally, to evaluate the expression of GRP78 during the progression of prostate cancer, we are currently characterizing the expression of GRP78 in a panel of human prostate cancer samples during different tumor stages, including organ-confined, locally advanced, and metastatic disease. Preliminary immunohistochemistry analysis suggests that GRP78 can be expressed even in early stage prostate cancer, that stage-specific upregulation of this target can occur, and that the expression of GRP78 is strong in metastatic disease (unpublished data). Overlay assays were again in agreement with such immunohis-
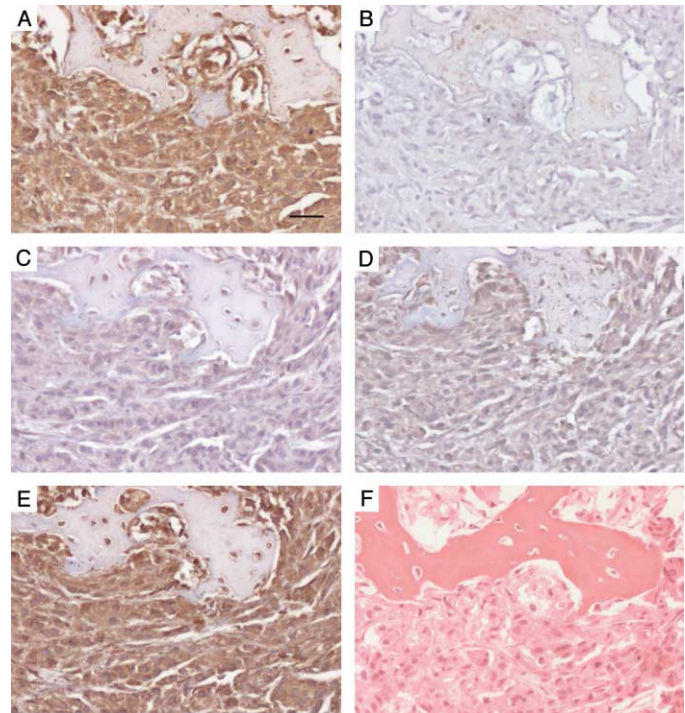
tochemistry observations. GRP78-targeted phage clones displaying either WIFPWIQL or WDLAWMFRLPVG peptides clearly stained prostate cancer tissue, whereas negative control phage showed only background staining; GRP78 expression verified with an anti-GRP78 antibody served as a positive control (Figure 8). Taken together, these results indicate that GRP78-based ligand-receptor interactions in the context of human prostate cancer progression are specific.

Discussion

Discovery of functional ligand-receptor systems is a critical step for the development of targeted therapies. Several lines of evidence have recently emerged to suggest that stress response proteins present on the surface of tumor cells may serve as molecular targets. First, global profiling of the cell surface proteome of tumor cells has disclosed a relative abundance of chaperone heat shock and glucose-regulated proteins (Shin et al., 2003). Second, fingerprinting the repertoire of antibodies derived from cancer patients with phage display random peptide libraries has identified a conformational mimic motif of one such glucose-regulated protein family member, GRP78, in prostate cancer. Antibodies against this peptide revealed cell surface
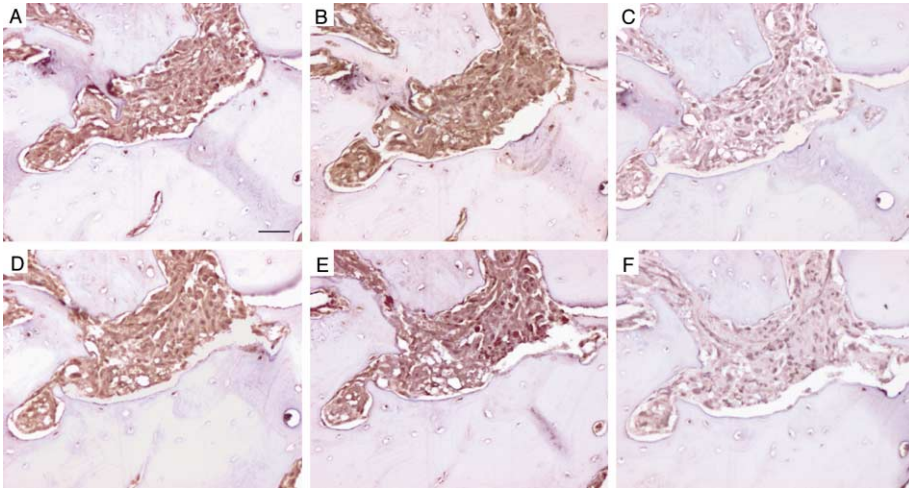
Figure 7. Inhibition of GRP78 binding phage staining by anti-GRP78 antibody

Serial tissue sections of bone marrow metastases from human prostate cancer were incubated with an anti-GRP78 antibody prior to adding the WIFPWIQL-phage, WDLAWMFRLPVG-phage, and negative control phage (fd-tet) to the sections. Strong staining was observed when the phage was applied with no antibody (**A** and **D**) or with negative control antibody (**B** and **E**). In contrast, marked reduction in phage staining was observed with anti-GRP78 antibody (**C** and **F**). Scale bar, 100 μm.

expression of GRP78 (Mintz et al., 2003). Third, GRP78 expressed on the surface of prostate cancer cells appears to mediate the signal transduction of α_2-macroglobulin (Misra et al., 2002), a plasma protease inhibitor that binds to prostate-specific antigen (PSA) as well (Kanoh et al., 2001). Fourth, we have shown that the humoral response elicited against the GRP78-mimic motif or against the native GRP78 strongly correlated with the development of androgen-independent disease and shorter overall survival in a large population of prostate cancer patients (Mintz et al., 2003). Fifth, GRP78 is overexpressed under conditions often found in tumors (such as ischemia, hypoxia, or glucose deprivation), hence its denomination as a glucose-regulated stress response protein that plays a central role in the general cellular defense mechanism that is referred to as the unfolded protein response (Kaufman, 1999; Lee, 2001; Reddy et al., 2003). Together, these observations led to efforts to evaluate GRP78 on the tumor cell membrane as a translational target for therapeutic intervention in the context of tumors such as metastatic prostate or breast cancers, currently incurable diseases.

Here, we designed and validated GRP78-based systems for ligand-directed targeting of solid tumors, in particular of prostate and breast cancer. We generated phage displaying GRP78 binding peptides by cloning the inserts WIFPWIQL and WDLAWMFRLPVG into a phage construct and then we studied the properties of these phage clones. First, WIFPWIQL-phage and WDLAWMFRLPVG-phage bound significantly more to GRP78 than to related and unrelated control proteins. We also showed that the synthetic WIFPWIQL and WDLAWMFRLPVG peptides inhibit binding of the corresponding phage in a dose-dependent manner, indicating that the interaction between the ligands and GRP78 is specific. Next, we established that WIFPWIQL-phage and WDLAWMFRLPVG-phage clones target GRP78 expressed on the cell membrane and are likely internalized by an active receptor-mediated process.

Moreover, to establish whether the GRP78 binding phage could home to human prostate cancer xenografts or mouse breast isogenic tumors in vivo, we administered the phage constructs and controls intravenously into tumor-bearing mice. At 24 hr, we observed localization of GRP78 binding phage into the tumors, with barely detectable phage localization to several control organs. The staining pattern observed in vivo indicates that GRP78-mediated targeted phage internalization occurred in tumor cells. In fact, selective accessibility based on the fenestrated and abnormal nature of tumor vasculature might allow for preferential targeting of tumor cells by GRP78-targeted proapoptotic peptides (Hashizume et al., 2000). We then tested the therapeutic properties of the GRP78 binding peptides linked to a proapoptotic motif (Arap et al., 2002b; Ellerby et al., 1999; Kolonin et al., 2004; Zurita et al., 2004) in vivo. Paradoxically, the GRP78-targeted proapoptotic peptides used in this work seem to promote programmed cell death in vitro in malignant as well as nonmalignant cells; in contrast, the apoptotic induction observed in vivo is clearly tumor specific. These data are relevant because they illustrate that the effects observed are not dependent on the origin of the tumor cells (human versus mouse), tumor type (prostate cancer versus breast cancer), or immune status of the host (nude mice versus immunocompetent mice). Antitumor effects of GRP78-targeted proapoptotic peptides were equally effective in both models: significant reduction in
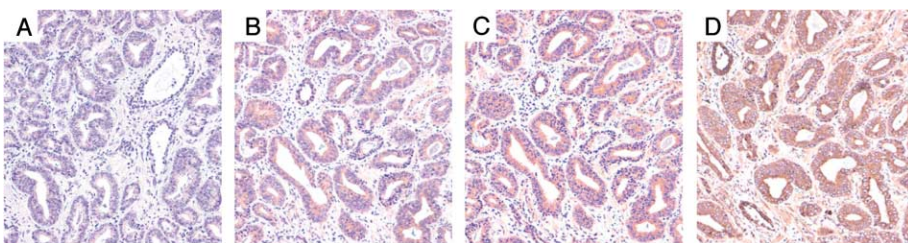

Figure 8. GRP78 binding phage overlay of primary human prostate cancer correlates to GRP78 expression

Relative to the weak staining observed with a negative control phage (**A**), strong staining was observed with either WDLAWMFRLPVG-phage (**B**), WIFPWIQL-phage (**C**), or anti-GRP78 antibody (**D**), which also served as a positive control for GRP78 expression.

tumor volumes when prostate cancer xenografts or murine breast isogenic tumors were treated with the targeted peptides relative to controls was observed. In agreement with such findings and the recent *GRP78* promoter studies of other investigators (Dong et al., 2004), we did not detect apoptosis induction in normal tissues upon administration of the GRP78-targeted proapoptotic peptides. Also, preliminary preclinical studies have shown that the maximum tolerated dose (MTD) for these peptides has not yet been reached (unpublished data), again reinforcing the notion that GRP78 is selectively targeted in our tumor models. Thus, this apparent limitation of in vitro models in this experimental system suggests that evaluation of GRP78-targeted treatment in mouse tumor models is more likely to be representative of clinically relevant aspects of disease in human cancer and is entirely consistent with the in vivo work of Dong et al. (2004).

Finally, GRP78 binding peptides also targeted human prostate cancer (both organ-confined and metastatic to the bone marrow), as shown by phage overlay assays (Arap et al., 2002a; Zurita et al., 2004). Serial sections from human prostate cancer at early or advanced stages yielded stronger staining when exposed to GRP78 binding phage clones than when exposed to control phage, reflecting the differential expression of GRP78 in the progression of prostate cancer. GRP78 binding phage clones abrogate the binding of an anti-GRP78 antibody, presumably due to the relatively large size of phage particles that can block access to the antigen. Consistently, an anti-GRP78 antibody also blocked the staining of GRP78 binding phage.

One might speculate on some additional aspects of the work presented here. Compared to other targets isolated by using phage display, a potential advantage of GRP78 is that its expression might allow not only ligand-directed but also transcriptional tumor targeting. It remains the focus of our ongoing studies to characterize whether specific tumor-associated GRP78 features (such as isoforms, chaperoned coreceptors, or differential activation states) might be present in the cell surface. Indeed, a recent study has shown that a fraction of GRP78 can exist as a transmembrane protein capable of trafficking to tumor cell surfaces (Reddy et al., 2003); thus, it is plausible that GRP78 might return to the cell surface after internalization occurs, as part of a dynamic process. In yet other lines of research, GRP78 has also been identified by phage display on the surfaces of endothelial cells in atheroma plaques (Liu et al., 2003) and of macrophages (Misra et al., 2002). These intriguing observations may open new GRP78-targeting applications in nonmalignant conditions with a stress response such as atherosclerotic and inflammatory diseases. If so, consideration should be given to selection of improved GRP78 ligands such as higher-affinity single-chain antibodies (Adams et al., 1998; Tarli et al., 1999; Viti et al., 1999), as an alternative or in addition to peptides or peptidomimetics.

In summary, these data establish GRP78 expressed in the cell surface as a tumor target in human prostate cancer, in line with the renewed interest in stress response proteins in prostate cancer (Cornford et al., 2000; Lebret et al., 2003a) and other urological tumors (Lebret et al., 2003b). Other membrane-associated chaperones (Shin et al., 2003) may also enable ligand-directed targeting. Indeed, it is possible that tumor-specific conformations might be found, enabling the development of high-affinity cell surface ligands against GRP78 and other stress response proteins. On a larger context, this study lends further support to the idea of exploiting the differential humoral immune response to human cancer (Mintz et al., 2003; Vidal et al., 2004) as a promising methodology for identifying targets for therapeutic intervention.

Experimental procedures

Cell culture and reagents
DU145 prostate cancer cells were purchased from the American Type Culture Collection (ATCC; Manassas, VA), and tissue culture was performed as described (Mickey et al., 1977). EF43-*fgf4* cells have been described (Deroanne et al., 1997; Hajitou et al., 2001, 2002; Marchiò et al., 2004). All soluble peptides were produced by Merrifield synthesis (AnaSpec, San Jose, CA and Genemed Synthesis, Inc., South San Francisco, CA). Unless otherwise specified, synthetic peptides with unrelated sequences were used as a negative control in binding experiments.

Generation of targeting vectors
DNA sequences encoding the GRP78 binding peptide motifs WIFPWIQL or WDLAWMFRLPVG (Blond-Elguindi et al., 1993) were cloned into SfiI-digested fUSE5 phage vectors (Smith and Scott, 1993). Briefly, 500 ng of each of the synthetic oligonucleotide templates corresponding to the displayed peptides (Sigma-Genosys, Woodlands, TX) were converted to double-stranded DNA by PCR amplification with the primer set 5′GTGAGCCGGCTGCCC3′ and 5′TTCGGCCCCAGCGGC3′ (Sigma-Genosys) and 2.5 U of Taq-DNA polymerase (Promega, Madison, WI) in 20 μl as follows: 94°C for 2 min, followed by 35 cycles at 94°C for 30 s, 60°C for 30 s, and 72°C for 30 s, followed by 72°C for 5 min. Double-stranded DNA sequences that contained BglI restriction sites in the insert-flanking regions were purified by using a QIAquick nucleotide removal kit (Qiagen, Hilden, Germany) and eluted from each QIAquick column (Qiagen) by 50 μl washes with ddH$_2$O. Oligonucleotides were digested with BglI for 2 hr at 37°C, repurified, and ligated into SfiI-digested fUSE5 vector. Plasmids were electroporated into MC1061 *E. coli*. DNA from each of the phage clones generated was PCR amplified to verify the correct insertion and nucleotide sequence.

Cell-free binding assay
GRP78, HSP70, HSP90 (all from Stressgen, Victoria, Canada), and BSA were immobilized on microtiter wells of 96-well plates overnight at 4°C. Wells were washed twice with phosphate-buffered saline (PBS), blocked with PBS containing 3% BSA for 1 hr at room temperature (RT), and incubated with 10^9 transducing units (TU) of WIFPWIQL-phage, WDLAWMFRLPVG-phage, or insertless control phage in 50 μl of PBS containing 1.5% BSA. After 2 hr at RT, wells were washed with PBS and bound phage clones were recovered by infection with host bacteria (log phase *E. coli* K91 kan; OD$_{600}$ ≈ 2). Aliquots of the bacterial culture were plated onto Luria-Bertani (LB) agar plates containing 40 μg/ml tetracycline and 100 μg/ml kanamycin (Smith and Scott, 1993; Pasqualini et al., 2001). Plates were incubated overnight at 37°C, and phage TU were counted in triplicate plates. Increasing molar concentrations of the corresponding synthetic peptides WIFPWIQL or WDLAWMFRLPVG were used to evaluate competitive inhibition of phage binding. All synthetic peptides were solubilized in a standard stock solution containing dimethylsulfoxide (DMSO) and diluted to working concentrations for the assays.

Cell surface binding assay
We used the biopanning and rapid analysis of selective interactive ligands (BRASIL) method (Giordano et al., 2001) to evaluate phage binding to intact cells. In brief, cultured human prostate cancer-derived DU145 cells were detached with ethylenediaminetetraacetate (EDTA) and resuspended in Dulbecco's modified Eagle's medium (DMEM) containing 1% BSA at 4×10^6 cells per ml. The cell suspension (50 μl) was incubated with 10^9 TU of WIFPWIQL-phage, WDLAWMFRLPVG-phage, or insertless control phage at 4°C in constant slow rotation. After 2 hr, the phage/cell mixture (aqueous phase) was gently transferred to the top of a nonmiscible organic phase (200 μl solution in a 400 μl Eppendorf tube) consisting of dibutyl phthalate: cyclohexane (9:1 [v:v], d = 1.03 g ml^{-1}) and centrifuged at 10,000 g for 10 min at 4°C. The tube was then snap frozen in liquid nitrogen, the bottom of the tube was sliced off, and the cell-phage pellet was isolated. Cell membrane bound phage were recovered by infection with the host bacteria (Giordano et al., 2001). A polyclonal rabbit anti-GRP78 antibody (Stressgen)

and an unrelated isotype control antibody at the same dilution, recombinant GRP78 (Stressgen), unrelated control proteins, and synthetic cognate or control peptides (each at 100 µg/ml) were used to evaluate competitive inhibition of phage binding.

Cell internalization assay

Cells were grown in tissue chamber slides (Lab-Tek II Chamber Slide System; Nalge Nunc International Corp., Naperville, IL), washed twice with PBS, incubated with 10^9 TU of WIFPWIQL-phage, WDLAWMFRLPVG-phage, or insertless control phage in DMEM containing 1% BSA at 37°C, and washed five times with PBS to remove unbound phage after 4 hr incubation. Bound phage clones to cell membranes were chemically eluted by rinsing cells with 20 mM glycine at pH 2.3. Next, cells were washed three times with PBS, fixed with PBS containing 4% paraformaldehyde (PFA) at RT for 15 min, washed with PBS, permeabilized with 0.2% Triton X-100, washed with PBS, and blocked with PBS containing 1% BSA. Cells were then incubated with a 1:200 dilution of the primary anti-M13 bacteriophage antibody (Amersham, Piscataway, NJ) in PBS containing 1% BSA at RT for 2 hr, washed with PBS, and incubated with a 1:200 dilution of a Cy^3-conjugated anti-rabbit secondary antibody in PBS containing 1% BSA for 1 hr at RT. Finally, cells were washed with PBS, fixed with PBS containing 4% PFA, mounted, and visualized in an optical fluorescence microscope.

Cell viability assay

A total of 2×10^4 cells per well were seeded in 96-well plates for 24 hr in DMEM containing 10% fetal bovine serum (FBS), incubated with increasing concentrations of the peptides WDLAWMFRLPVG-GG-$_D$(KLAKLAK)$_2$ or WDLAWMFRLPVG and $_D$(KLAKLAK)$_2$ in 60 µl DMEM containing 1% FBS for 2 hr at 37°C and with or without 20 mM sodium azide (NaN$_3$). After 2 hr, cell viability was measured with a cell proliferation detection reagent (WST-1; Roche, Mannheim, Germany). All samples were performed in triplicates.

Establishment of tumor-bearing mice

Immunodeficient male athymic nu/nu (nude) mice were commercially obtained (Harlan-Sprague-Dawley, Indianapolis, IN). Prostate cancer xenografts were established by subcutaneous administration of human DU145 cells (10^6 cells in 200 µl DMEM) into the subcutaneous tissue of the nude mice. Immunocompetent female Balb/c mice bearing mouse EF43-*fgf4*-derived breast tumors were established as described (Deroanne et al., 1997; Hajitou et al., 2001, 2002; Marchiò et al., 2004). The Internal Animal Care and Use Committee of the University of Texas M.D. Anderson Cancer Center (UTMDACC) reviewed and approved all animal experimentation.

Tumor targeting in vivo

In vivo targeting experiments with phage were performed as described (Arap et al., 1998; Koivunen et al., 1999; Kolonin et al., 2004; Marchiò et al., 2004; Pasqualini et al., 2001). Briefly, either male nude mice bearing size-matched human DU145 xenografts or immunocompetent female Balb/c female mouse bearing EF43-*fgf4*-derived breast tumors were deeply anesthetized and injected intravenously (tail vein) with 10^{10} TU of WIFPWIQL-phage, WDLAWMFRLPVG-phage, RGD-4C phage (positive control), or fd-tet phage (negative control) in vehicle (DMEM). Cohorts of three mice with size-matched tumors received each set of phage clones. After 24 hr, tumor-bearing mice were perfused through the heart with 20 ml of 4% PFA. Tumor and control organs were dissected from each mouse and fixed in PBS containing 4% PFA for 24 hr. Finally, tissues were paraffin embedded and sectioned into 5 µm specimens for phage staining as described (Pasqualini et al., 2001).

Immunohistochemical analysis

Immunohistochemistry on sections of fixed paraffin-embedded mouse tissues was performed with the LSAB+ peroxidase kit (DAKO, Carpinteria, CA). Briefly, slides were deparaffinized and rehydrated with xylene and graded alcohols, blocked for endogenous peroxidases, and antigen retrieved in a microwave oven by treatment with an antigen retrieval solution (DAKO). Slides were blocked for nonspecific protein binding, and a rabbit anti-bacteriophage primary antibody (Sigma) was added (150 µl at 1:500 dilution). After 1 hr, slides were washed three times with 20 mM Tris-buffered saline containing 0.1% Tween 20 (TBST), and peroxidase-conjugated anti-rabbit secondary antibody was added. The slides were washed again three times with TBST and developed with the substrate chromogen 3,3′-Diaminobenzi-

dine (DAB; DAKO). Counterstaining was achieved by a 20 s immersion in 100% hematoxylin, and the slides were dehydrated (with graded alcohols and xylene) and mounted. All sections and controls from each specimen were included in simultaneous staining runs to minimize experimental variability.

Targeted proapoptotic peptide treatment of tumor-bearing mice

Cohorts of tumor-bearing mice were size matched and divided into groups (n = 7 each), and treatments started when mean tumor volumes reached ~200 mm^3; the weights of mice were also similar (<5% variation) within each treatment cohort. Two GRP78-targeting peptides (WIFPWIQL or WDLAWMFRLPVG) were each synthesized as a chimera with the proapoptotic motif $_D$(KLAKLAK)$_2$ and used as therapy in tumor-bearing mice while control tumor-bearing mice received a corresponding equimolar mixture of either unconjugated WIFPWIQL plus $_D$(KLAKLAK)$_2$ or unconjugated WDLAWMFRLPVG plus $_D$(KLAKLAK)$_2$. Mice were deeply anesthetized, and tumor volumes were measured as described (Arap et al., 1998; Koivunen et al., 1999; Marchiò et al., 2004; Pasqualini et al., 2001). Therapeutic and control peptides were systemically administered (tail vein) at 300 µg/dose/mouse in 200 µl of vehicle (DMEM) weekly for a period of 4 weeks.

Phage overlay and competition assay on human tissue samples

Immunohistochemistry on sections of fixed human paraffin-embedded bone metastases from prostate cancer patients was performed with LSAB+ peroxidase kit (DAKO). Human samples of metastatic prostate cancer patients (n = 6) were obtained from the University of São Paulo Medical School, Brazil. Sections (5 µm) were deparaffinized, rehydrated, and blocked for endogenous peroxidases and for nonspecific protein binding. An anti-GRP78 goat polyclonal antibody (C-20, sc-1051; Santa Cruz Biotechnology, Santa Cruz, CA) and an unrelated control goat polyclonal isotype antibody (goat IgG-reagent grade; Sigma, St. Louis, MO) at the same immunoglobulin concentration were used to evaluate competitive inhibition of phage binding. Tissue sections were incubated with media alone, anti-GRP78 antibody, or control antibody at the same immunoglobulin concentration for 1 hr at RT. Next, 2×10^9 TU of WIFPWIQL-phage, WDLAWMFRLPVG-phage, or negative control phage were incubated for 2 hr at RT. An anti-bacteriophage antibody (Sigma) was added to the slides (150 µl of a 1:500 dilution) and incubated for 1 hr at RT. After three washes with TBST, the peroxidase-conjugated anti-rabbit secondary antibody was added. Slides were washed three times with TBST, developed with DAB, counterstained by a 20 s immersion in 100% hematoxylin, dehydrated, and mounted. To test whether the phage would block anti-GRP78 antibody staining, we proceeded as follows. First, after deparaffinization, rehydration, protein, and peroxidase blockages, 2×10^9 TU of WIFPWIQL-phage, WDLAWMFRLPVG-phage, negative control phage, or media alone were added to the slides and incubated for 2 hr. Next, anti-GRP78 antibody or control antibody at an equivalent immunoglobulin concentration was added to the slides and incubated for 1 hr at RT. Slides were washed three times with TBST, and a peroxidase-conjugated secondary antibody was added. After three washes, development was achieved with the DAB substrate. Slides were counterstained by hematoxylin, dehydrated, and mounted. The Institutional Review Board (IRB) of the University of São Paulo Medical School reviewed and approved all experimentation in patient-derived samples.

Statistical analysis

Experimental results are expressed as mean ± standard errors of the mean (SEM) of triplicate plates. Statistical significance was determined by Student's t tests.

References

Adams, G.P., Schier, R., Marshall, K., Wolf, E.J., McCall, A.M., Marks, J.D., and Weiner, L.M. (1998). Increased affinity leads to improved selective tumor delivery of single-chain Fv antibodies. Cancer Res. 58, 485–490.

Arap, W., Pasqualini, R., and Ruoslahti, E. (1998). Cancer treatment by targeted drug delivery to tumor vasculature in a mouse model. Science 279, 377–380.

Arap, W., Kolonin, M.G., Trepel, M., Lahdenranta, J., Cardó-Vila, M., Giordano, R.J., Mintz, P.J., Ardelt, P.U., Yao, V.J., Vidal, C.I., et al. (2002a). Steps toward mapping the human vasculature by phage display. Nat. Med. 8, 121–127.

Arap, W., Haedicke, W., Bernasconi, M., Kain, R., Rajotte, D., Krajewski, S., Ellerby, H.M., Bredesen, D.E., Pasqualini, R., and Ruoslahti, E. (2002b). Targeting the prostate for destruction through a vascular address. Proc. Natl. Acad. Sci. USA 99, 1527–1531.

Beere, H.M., Wolf, B.B., Cain, K., Mosser, D.D., Mahboubi, A., Kuwana, T., Tailor, P., Morimoto, R.I., Cohen, G.M., and Green, D.R. (2000). Heat-shock protein inhibits apoptosis by preventing recruitment of procaspase-9 to the apaf-1 apoptosome. Nat. Cell Biol. 2, 469–475.

Blond-Elguindi, S., Cwirla, S.E., Dower, W.J., Lipshutz, R.J., Sprang, S.R., Sambrook, J.F., and Gething, M.J. (1993). Affinity panning of a library of peptides displayed on bacteriophages reveals the binding specificity of BiP. Cell 75, 717–728.

Cornford, P.A., Dodson, A.R., Parsons, K.F., Desmond, A.D., Woolfenden, A., Fordham, M., Neoptolemos, J.P., Ke, Y., and Foster, C.S. (2000). Heat shock protein expression independently predicts clinical outcome in prostate cancer. Cancer Res. 60, 7099–7105.

Deroanne, C.F., Hajitou, A., Calberg-Bacq, C.M., Nusgens, B.V., and Lapiere, C.M. (1997). Angiogenesis by fibroblast growth factor 4 is mediated through an autocrine up-regulation of vascular endothelial growth factor expression. Cancer Res. 50, 5531–5536.

Dong, D., Dubeau, L., Bading, J., Nguyen, K., Luna, M., Yu, H., Gazit-Bornstein, G., Gordon, E.M., Hall, F.L., et al. (2004). Spontaneous and controllable activation of suicide gene expression driven by the stress-induced Grp78 promoter resulting in eradication of sizable human tumors. Hum. Gene Ther. 15, 553–561.

Ellerby, H.M., Arap, W., Ellerby, L.M., Kain, R., Andrusiak, R., Rio, G.D., Krajewski, S., Lombardo, C.R., Rao, R., Ruoslahti, E., et al. (1999). Anti-cancer activity of targeted proapoptotic peptides. Nat. Med. 5, 1032–1038.

Giordano, R.J., Cardó-Vila, M., Lahdenranta, J., Pasqualini, R., and Arap, W. (2001). Biopanning and rapid analysis of selective interactive ligands. Nat. Med. 7, 1249–1253.

Hajitou, A., Souni, N.E., Devy, L., Debrus-Grignet, C., Lewalle, J.M., Hong, L., Deroanne, C.F., Lu, H., Colige, A., Nusgens, B.V., et al. (2001). Down-regulation of vascular endothelial growth factor by tissue inhibitor of metallo-proteinase-2: effect on in vivo mammary tumor growth and angiogenesis. Cancer Res. 61, 3450–3457.

Hajitou, A., Grignet, C., Devy, L., Berndt, S., Blacher, S., Deroanne, C.F., Bajou, K., Fong, T., Chiang, Y., Foidart, J.M., et al. (2002). The antitumoral effect of endostatin and angiostatin is associated with a down-regulation of vascular endothelial growth factor expression in tumor cells. FASEB J. 16, 1802–1804.

Hashizume, H., Baluk, P., Morikawa, S., McLean, J.W., Thurston, G., Roberge, S., Jain, R.K., and McDonald, D.M. (2000). Openings between defective endothelial cells explain tumor vessel leakiness. Am. J. Pathol. 156, 1363–1380.

Jamora, C., Dennert, G., and Lee, A.S. (1996). Inhibition of tumor progression by suppression of stress protein GRP78/BiP induction in fibrosarcoma B/C10ME. Proc. Natl. Acad. Sci. USA 93, 7690–7694.

Javadpour, M.M., Juban, M.M., Lo, W.C., Bishop, S.M., Alberty, J.B., Cowell, S.M., Becker, C.L., and McLaughlin, M.L. (1996). De novo antimicrobial peptides with low mammalian cell toxicity. J. Med. Chem. 39, 3107–3113.

Kamal, A., Thao, L., Sensintaffar, J., Zhang, L., Boehm, M.F., Fritz, L.C., and Burrows, F.J. (2003). A high-affinity conformation of Hsp90 confers tumour selectivity on Hsp90 inhibitors. Nature 425, 407–410.

Kanoh, Y., Ohtani, N., Mashiko, T., Ohtani, S., Nishikawa, T., Egawa, S., Baba, S., and Ohtani, H. (2001). Levels of $\alpha 2$ macroglobulin can predict bone metastases in prostate cancer. Anticancer Res. 21, 551–556.

Kaufman, R.J. (1999). Stress signaling from the lumen of the endoplasmic reticulum: coordination of gene transcriptional and translational controls. Genes Dev. 13, 1211–1233.

Koivunen, E., Arap, W., Valtanen, H., Rainisalo, A., Medina, O.P., Heikkila, P., Kantor, C., Gahmberg, C.G., Salo, T., Konttinen, Y.T., et al. (1999). Tumor targeting with a selective gelatinase inhibitor. Nat. Biotechnol. 17, 768–774.

Kolonin, M.G., Saha, P.K., Chan, L., Pasqualini, R., and Arap, W. (2004). Reversal of obesity by targeted ablation of adipose tissue. Nat. Med. 10, 625–632.

Koong, A.C., Chen, E.Y., Lee, A.S., Brown, J.M., and Giaccia, A.J. (1994). Increased cytotoxicity of chronic hypoxic cells by molecular inhibition of GRP78 induction. Int. J. Radiat. Oncol. Biol. Phys. 28, 661–666.

Lebret, T., Watson, R.W., and Fitzpatrick, J.M. (2003a). Heat shock proteins: their role in urological tumors. J. Urol. 169, 338–346.

Lebret, T., Watson, R.W., Molinie, V., O'Neill, A., Gabriel, C., Fitzpatrick, J.M., and Botto, H. (2003b). Heat shock proteins HSP27, HSP60, HSP70, and HSP90: expression in bladder carcinoma. Cancer 98, 970–977.

Lee, A.S. (2001). The glucose-regulated proteins: stress induction and clinical applications. Trends Biochem. Sci. 26, 504–510.

Li, L.J., Li, X., Ferrario, A., Rucker, N., Liu, E.S., Wong, S., Gomer, C.J., and Lee, A.S. (1992). Establishment of a Chinese hamster ovary cell line that expresses grp78 antisense transcripts and suppresses A23187 induction of both GRP78 and GRP94. J. Cell. Physiol. 153, 575–582.

Liu, C., Bhattacharjee, G., Boisvert, W., Dilley, R., and Edgington, T. (2003). In vivo interrogation of the molecular display of atherosclerotic lesion surfaces. Am. J. Pathol. 163, 1859–1871.

Marchiò, S., Lahdenranta, J., Schlingemann, R.O., Valdembri, D., Wesseling, P., Arap, M.A., Hajitou, A., Ozawa, M.G., Trepel, M., Giordano, R.J., et al. (2004). Aminopeptidase A is a functional target in angiogenic blood vessels. Cancer Cell 5, 151–162.

Mickey, D.D., Stone, K.R., Wunderli, H., Mickey, G.H., Vollmer, R.T., and Paulson, D.F. (1977). Heterotransplantation of a human prostatic adenocarcinoma cell line in nude mice. Cancer Res. 37, 4049–4058.

Mintz, P.J., Kim, J., Do, K.A., Wang, X., Zinner, R.G., Cristofanilli, M., Arap, M.A., Hong, W.K., Troncoso, P., Logothetis, C.J., et al. (2003). Fingerprinting the circulating repertoire of antibodies from cancer patients. Nat. Biotechnol. 21, 57–63.

Misra, U.K., Gonzalez-Gronow, M., Gawdi, G., Hart, J.P., Johnson, C.E., and Pizzo, S.V. (2002). The role of Grp 78 in $\alpha 2$-macroglobulin-induced signal transduction. Evidence from RNA interference that the low-density lipoprotein receptor-related protein is associated with, but not necessary for, GRP 78-mediated signal transduction. J. Biol. Chem. 277, 42082–42087.

Miyake, H., Hara, I., Arakawa, S., and Kamidono, S. (2000). Stress protein GRP78 prevents apoptosis induced by calcium ionophore, ionomycin, but not by glycosylation inhibitor, tunicamycin, in human prostate cancer cells. J. Cell. Biochem. 77, 396–408.

Neckers, L., and Lee, Y.S. (2003). Cancer: the rules of attraction. Nature 425, 407–410.

Nicchitta, C.V. (2003). Re-evaluating the role of heat-shock protein-peptide interactions in tumour immunity. Nat. Rev. Immunol. 3, 427–432.

Pasqualini, R., Arap, W., Rajotte, D., and Ruoslahti, E. (2001). In vivo selection

of phage-display libraries. In Phage Display. A Laboratory Manual, C.F. Barbas III, D.R. Burton, J.K. Scott, and G.J. Silverman, eds. (Cold Spring Harbor, NY: Cold Spring Harbor Laboratory Press), pp. 1–24.

Ravagnan, L., Gurbuxani, S., Susin, S.A., Maisse, C., Daugas, E., Zamzami, N., Mak, T., Jaattela, M., Penninger, J.M., Garrido, C., et al. (2001). Heat-shock protein 70 antagonizes apoptosis-inducing factor. Nat. Cell Biol. *3*, 839–843.

Reddy, R.K., Mao, C., Baumeister, P., Austin, R.C., Kaufman, R.J., and Lee, A.S. (2003). Endoplasmic reticulum chaperone protein GRP78 protects cells from apoptosis induced by topoisomerase inhibitors: role of ATP binding site in suppression of caspase-7 activation. J. Biol. Chem. *278*, 20915–20924.

Schmid, S.L., and Carter, L.L. (1990). ATP is required for receptor-mediated endocytosis in intact cells. J. Cell Biol. *111*, 2307–2318.

Shin, B.K., Wang, H., Yim, A.M., Le Naour, F., Brichory, F., Jang, J.H., Zhao, R., Puravs, E., Tra, J., Michael, C.W., et al. (2003). Global profiling of the cell surface proteome of cancer cells uncovers an abundance of proteins with chaperone function. J. Biol. Chem. *278*, 7607–7616.

Smith, G.P., and Scott, J.K. (1993). Libraries of peptides and proteins displayed on filamentous phage. Methods Enzymol. *217*, 228–257.

Sugawara, S., Takeda, K., Lee, A., and Dennert, G. (1993). Suppression of stress protein GRP78 induction in tumor B/C10ME eliminates resistance to cell mediated cytotoxicity. Cancer Res. *53*, 6001–6005.

Tarli, L., Balza, E., Viti, F., Borsi, L., Castellani, P., Berndorff, D., Dinkelborg, L., Neri, D., and Zardi, L. (1999). A high-affinity human antibody that targets tumoral blood vessels. Blood *94*, 192–198.

Vidal, C.I., Mintz, P.J., Manenti, L., Broaddus, R., Lu, K., Ellis, L.M., Gershenson, D.M., Giavazzi, R., Liu, J., Arap, W., et al. (2004). An HSP90-mimic peptide revealed by fingerprinting the pool of antibodies from ovarian cancer patients. Oncogene, in press.

Viti, F., Tarli, L., Giovannoni, L., Zardi, L., and Neri, D. (1999). Increased binding affinity and valence of recombinant antibody fragments lead to improved targeting of tumoral angiogenesis. Cancer Res. *59*, 347–352.

Zurita, A.J., Troncoso, P., Cardó-Vila, M., Logothetis, C.J., Pasqualini, R., and Arap, W. (2004). Combinatorial screenings in patients: the interleukin-11 receptor α as a candidate target in the progression of human prostate cancer. Cancer Res. *64*, 435–439.